A Direct Modulation Index Control Strategy for Three-Phase Vienna Rectifier at Light Load

Yipei Wang, *Member, IEEE*, Sang-Hyeok Lee, Hyeon-Uk Go, Min-Seong Kim, Guangxu Zhou, and Sung-Jun Park, *Member, IEEE*

***Abstract*—The three-phase Vienna rectifier suffers from the inherent problem of increased or unstable output voltage on the dc side at light loads. In this article, a light-load state judgment criterion is derived based on the Vienna equivalent model. A direct modulation index control strategy is further proposed to optimize the light-load performance, which is implemented by proportional control and voltage feedforward. The proposed method significantly reduces the duty cycle by directly modifying the modulation index, ensuring that, at any given time, only one phase switch is in pulsewidth modulation mode at most, which reduces the energy transfer path and simplifies the operating modes. To verify the validity of the proposed strategy, a Vienna rectifier prototype is designed and built. The proposed strategy improves the dc voltage stability and dynamic characteristics under light load at the cost of input current harmonics. The experimental results show that the dc voltage ripple rate is less than 0.25% in steady state and the voltage overshoot is less than 1.7% in transient.**

***Index Terms*—Duty cycle, light load, modulation index, Vienna rectifier, voltage fluctuation.**

I. Introduction

THE three-phase Vienna rectifier, as a three-level converter, due to its advantages of high efficiency, high power density, and cost-effectiveness [1], [2], [3], is widely employed in several industrial applications, including electrical vehicle (EV) chargers [4], power factor correction (PFC) [5], telecommunication power systems [6], and medical X-ray systems [7].

Received 23 January 2025; revised 29 March 2025; accepted 26 April 2025. Date of publication 29 April 2025; date of current version 30 June 2025. This work was supported in part by Shandong Province "Double-Hundred Talent Plan" under Grant WST2024010, in part by the Korea Institute of Energy Technology Evaluation and Planning grant funded by the Korean Government (MOTIE) under Grant 20222020900080, in part by Key Technology Research Project in Qingdao under Grant 25-1-1-gjgg-4-gx, and in part by the Gwangju Jeonnam Local Energy Cluster Human Resources Development of the Korea Institute of Energy Technology Evaluation and Planning grant funded by the Korea Government Ministry of Trade, Industry, and Energy under Grant 20214000000560. Recommended for publication by Associate Editor C.N.M. Ho. *(Corresponding author: Sung-Jun Park.)*

Yipei Wang and Guangxu Zhou are with the Institute of Automation, Qilu University of Technology (Shandong Academy of Sciences), Jinan 250014, China (e-mail: wangyipei@qlu.edu.cn; zhougx@sdas.org).

Sang-Hyeok Lee is with Korea Electronics Technology Institute, Gwangju 61011, South Korea (e-mail: klsh@keti.re.kr).

Hyeon-Uk Go, Min-Seong Kim, and Sung-Jun Park are with the Department of Electrical Engineering, Chonnam National University, Gwangju 61186, South Korea (e-mail: yud01065@jnu.ac.kr; alstjd0415@jnu.ac.kr; sjpark1@jnu.ac.kr).

Color versions of one or more figures in this article are available at https://doi.org/10.1109/TPEL.2025.3565578.

Digital Object Identifier 10.1109/TPEL.2025.3565578

In Vienna rectifiers, the dc-side output voltage stability and ac-side current quality are significant performance indicators [8], and their priority depends on specific application scenarios and system performance requirements. The Vienna rectifiers are generally followed by a dc/dc converter or directly connected to a dc load. Therefore, for the above applications, the stability of the dc-side output voltage at light-load conditions is essential [9], [10]. Such systems often operate in low-power standby mode for extended periods, especially at night when user traffic is minimal. In addition, for EV chargers, which require constant voltage (CV) charging functions, the voltage fluctuation leads to limited CV function and lower system performance and reliability [11]. The boost PFC and dc voltage control functions are not unavailable with the three-phase diode rectification. High current quality on the ac side can reduce the grid harmonics and improve the power system stability [12]. Under light-load conditions, if the dc-side voltage fluctuates greatly or the overvoltage protection is triggered, which poses a potential threat to operating safety, then the discussion of power quality becomes meaningless. The trade-off is that for high-power industrial applications, power quality is prioritized to reduce harmonic effects. While for light-load and high-reliability applications, dc-side voltage stability over the full-load range should be emphasized [13], [14].

However, it is worth noting that the Vienna rectifier is a unidirectional energy transfer converter, and voltage control is difficult at light loads, the main reasons are as follows [14], [15], [16], [17].

1) At light loads, the output power and inertia are low. For the *dq* rotating coordinate system, the accuracy and sensitivity of the controller are not sufficient to provide a fast dynamic response and stable voltage control.
2) The rectifier enters the discontinuous conduction mode (DCM), and the inductor current drops to zero, which means that no energy is transferred to the output during some switching cycles.
3) The energy pulsations increase, and the dc-side capacitor suffers from uncontrolled periodic charging and discharging, which can cause voltage fluctuation and overshoot.
4) The optimal parameters for the PI controller are different under light-load and normal state.

However, as the controller is designed for continuous conduction mode (CCM), the voltage cannot be regulated correctly in DCM. Therefore, the corresponding methods should be taken to suppress voltage fluctuation and avoid system overvoltage protection.

There have been relatively few investigations into improving the light-load performance of the three-phase Vienna rectifiers. The typical control strategy for the three-phase Vienna rectifiers is PI control in a synchronous rotating coordinate system, which is based on CCM, so it is difficult to achieve stable control of the output voltage at light loads. In [7], a control scheme based on an exact analytical solution of the DCM duty cycle is proposed, the priority is to prevent input current distortion under light load, rather than dc voltage stability. This approach does not require current measurements or an actual feedback control loop because the feedforward calculation of the duty cycle is based on the actual current reference amplitude [18]. However, there is a significant overshoot in dc voltage when switching to light load, and the characteristics of steady state under light load are not discussed. A burst-mode control is proposed in [13], which employs hysteresis loop control to determine the triggering or not of the driver, thus limiting the output voltage to the hysteresis loop range. However, whether the hysteresis loop control is applied to the dc voltage or the voltage loop output, the dc voltage ripple and dynamic characteristics can be further improved. The burst-mode control is also employed in [19] to reduce the loop current losses and improve the efficiency, but it can only guarantee a limited voltage stabilization capability. Based on the instantaneous input voltage levels, phase angles, and zero quantities, a minimum power characteristic adaptive control strategy based on CCM and DCM boundary is proposed in [16]. However, the dc-link voltage is deviated, and there is a lack of experimental data to support the method. This method is also regarded as feedforward control, which mainly emphasizes the difference between the theoretical voltage based on the duty cycle and the actual voltage under DCM [14]. Based on the analysis of boundary conduction-mode control methods, Chen et al. [20] introduced a variable feedback control to limit the duty cycle under no-load conditions. For bipolar dc bus Vienna rectifier, the dc offset of the neutral point voltage is more pronounced at light loads, and a vector phase angle difference optimization strategy is presented in [21]. The proposed strategy reduces the dc offset of the neutral voltage at the cost of input current harmonics and dc-side voltage fluctuations under light-load conditions, but the focus is not on dc voltage stability. In [22], an optimal switching sequence model predictive control (OSS-MPC) is proposed. The OSS-MPC is responsible for current control, and dc voltage regulation and neutral voltage balancing are realized by PI control and redundant vector preselection techniques, respectively. Compared with the traditional optimal switching vector MPC, although the proposed strategy can control the dc voltage stably under light loads, the voltage overshoot and transition time are still too large, and its effectiveness under very light loads requires experimental verification.

To address the problem of dc voltage runaway under light load of the Vienna rectifier, this article proposes a direct modulation index control strategy. The proposed strategy improves the dc voltage stability and dynamic characteristics under light load at the cost of input current harmonics. Several critical contributions are made as follows.

1) The DCM critical load value is derived according to the Vienna equivalent model. The causes and phenomena of voltage runaway under light load are described, and the light-load state criterion is analyzed.
2) The effect of the modulation index on the duty cycle and drive signal is analyzed, and the proposed light-load control strategy reduces the duty cycle by directly adjusting the modulation index. The design considerations and tradeoffs are discussed. The proposed method is implemented by proportional control and voltage feedforward, which can ensure that, at any time, at most, only one phase is in pulsewidth modulation (PWM) mode. This control strategy minimizes the energy transfer path while simplifying operating modes and control complexity.
3) To verify the validity of the proposed strategy, a Vienna rectifier prototype is designed and built. The proposed strategy's performance is evaluated through simulation and experimentation. Compared with traditional methods, the proposed light-load control strategy effectively improves dc voltage stability under steady-state and dynamic conditions.

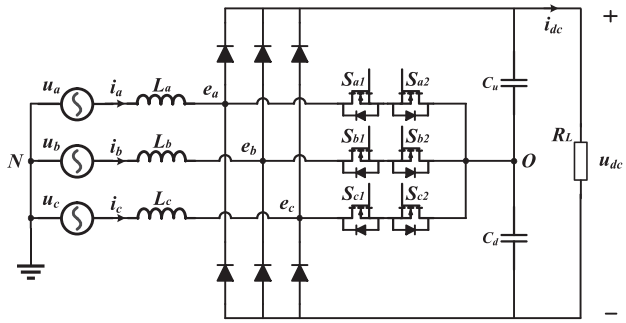

Fig. 1. Topology of the Vienna rectifier.

The rest of this article is organized as follows. Section II introduces the Vienna equivalent model and derives the critical load current for the light-load state. Section III discusses the proposed direct modulation index control strategy and its operating principle. Section IV verifies the validity of the proposed strategy through experiments. Finally, Section V concludes this article.

II. Three-Phase Vienna Rectifier Operating Principle

A. Equivalent Model

The topology of the Vienna rectifier is shown in Fig. 1. u_x ($x = a,b,c$) represents the three-phase grid voltage, i_x represents the three-phase grid current, and e_x represents the bridge midpoint voltage. L_x represents the three-phase boost inductor, $u_{\rm dc}$ is the dc-side output voltage, R_L is the load, and N is the ac voltage midpoint. The dc-side capacitor consists of two capacitors C_u and C_d connected in series, with each capacitor withstanding half the voltage of $u_{\rm dc}$.

The three-phase rectifier bridge employs diodes, and for each phase, the bidirectional switch consists of two switch devices S_{x1} and S_{x2} connected in reverse series, thus enabling bidirectional current flow. The switches in a typical Vienna rectifier are hard switched, not soft switched. The two switches share a common

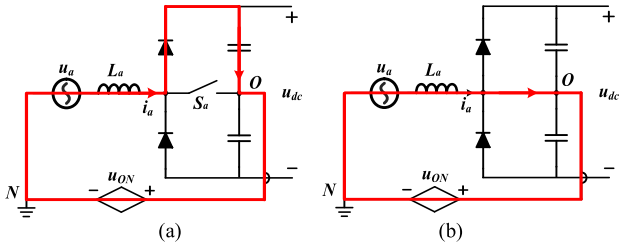

Fig. 2. Operating principle of the single-phase Vienna rectifier (a-phase positive half cycle). (a) When S_a is turned OFF. (b) When S_a is turned ON.

drive signal, eliminating the requirement for deadtime, which is further simplified as a single bidirectional switch S_x ($x = a,b,c$). The three bidirectional switches are all connected to the dc-side midpoint O to achieve a three-level output. By controlling the three bidirectional switches, it is possible to regulate the current in each phase to implement PFC. Since the three-phase Vienna rectifier can be decoupled, the a-phase is taken as an example in this article to illustrate its operating principle and mathematical model. The following assumptions are made for Vienna to facilitate derivation and simplification.

1) The losses of all switching devices are not considered.
2) The three-phase grid voltage is ideal and balanced, and the system is operating in steady state.
3) The switching frequency is much higher than the grid frequency.
4) The output voltages across the two capacitors on the dc side are balanced.

The circuit voltage expression for a three-phase Vienna rectifier is given by

$$\begin{cases} L\frac{di_a}{dt} = u_a - Ri_a - e_{aO} - u_{\mathrm{ON}} = u_a - Ri_a - e_a \\ L\frac{di_b}{dt} = u_b - Ri_b - e_{bO} - u_{\mathrm{ON}} = u_b - Ri_b - e_b \\ L\frac{di_c}{dt} = u_c - Ri_c - e_{cO} - u_{\mathrm{ON}} = u_c - Ri_c - e_c \end{cases} \tag{1}$$

where R is the line resistance of each phase, and $e_{xO}(x = a, b, c)$ is the voltage between e_x and O. u_{ON} is the voltage between O and N. e_{xO} is determined by the switching state and current polarity, which can be expressed as follows:

$$\begin{cases} e_{aO} = (1 - S_a)\,\mathrm{sgn}\,(i_a)\,\frac{u_{\mathrm{dc}}}{2} \\ e_{bO} = (1 - S_b)\,\mathrm{sgn}\,(i_b)\,\frac{u_{\mathrm{dc}}}{2} \\ e_{cO} = (1 - S_c)\,\mathrm{sgn}\,(i_c)\,\frac{u_{\mathrm{dc}}}{2} \end{cases} \tag{2}$$

where $\mathrm{sgn}(i_x)$ distinguishes the current direction, and S_x is the switching function, which can be defined as follows:

$$\mathrm{sgn}\,(i_x) = \begin{cases} 1 & i_x > 0 \\ -1 & i_x < 0 \end{cases} S_x = \begin{cases} 1 & S_x\mathrm{ON} \\ 0 & S_x\mathrm{OFF}. \end{cases} \tag{3}$$

When the three-phase grid is symmetrical, the sum of the three-phase voltages and currents is zero, according to (1) and (2)

$$u_{\mathrm{ON}} = -\frac{e_{aO} + e_{bO} + e_{cO}}{3}. \tag{4}$$

Fig. 2 describes the operating principle of the a-phase Vienna rectifier during the positive half cycle of u_a. When the a-phase switch S_a is turned OFF, L_a releases energy, and i_a decreases linearly, as shown by the red path in Fig. 2(a). When the switch S_a is turned ON, L_a stores energy, and i_a increases, as shown by the red path in Fig. 2(b). In the case of a three-phase balance, the common-mode voltage u_{ON} can be represented by a CV source. The rectifier regulates the input current through the inductor and PWM, which provides a boost characteristic. The operating principle is similar for the negative half cycle of u_a. Thus, the single-phase Vienna rectifier can be equivalent to a boost converter, as shown in Fig. 3. Compared with a three-phase four-wire system, the system mathematical model is similar, with the difference being the introduction of a CV source in the boost converter. However, the analysis process and control method are identical.

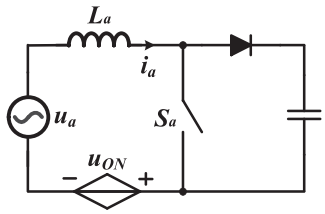

Fig. 3. Equivalent circuit of the single-phase Vienna rectifier.

B. DCM and Light-Load Condition

As the load current decreases, the Vienna rectifier will transition from CCM to DCM. According to Fig. 3, the average of the a-phase inductor current in one switching period T_s can be expressed as follows:

$$\langle i_a \rangle_{T_s} = \frac{\langle u_a - u_{\mathrm{ON}} \rangle_{T_s}}{(1 - d_a)^2 R_L} \tag{5}$$

where d_a is the duty cycle of the switch S_a. The ripple amplitude of the inductor current is given as follows:

$$\Delta i_a = \frac{u_a - u_{\mathrm{ON}}}{L_a} d_a T_s. \tag{6}$$

The conditions for a-phase to operate in CCM can be obtained as follows:

$$\frac{u_a - u_{\mathrm{ON}}}{(1 - d_a)^2 R_L} > \frac{\Delta i_a}{2} = \frac{u_a - u_{\mathrm{ON}}}{2L_a} d_a T_s. \tag{7}$$

The above equation can be further simplified as follows:

$$\begin{cases} J > J_{\mathrm{cri}} & \mathrm{CCM} \\ J < J_{\mathrm{cri}} & \mathrm{DCM} \end{cases}$$

$$\text{where } J = \frac{2L_a}{R_L T_s} \quad J_{\mathrm{cri}}\,(d_a) = (1 - d_a)^2 d_a. \tag{8}$$

J_{cri} is the criterion for determining the boundary mode, and the maximum value of J_{cri} is $J_{\mathrm{cri}}(\frac{1}{3}) = \frac{4}{27}$. It can be seen that the criterion is independent of the voltage and is the same for three-wire and four-wire systems. The function relationship between J_{cri} and the duty cycle is shown in Fig. 4. Equation (8) can be expressed in terms of a resistor as follows:

$$\begin{cases} R_L < R_{\mathrm{cri}} & \mathrm{CCM} \\ R_L > R_{\mathrm{cri}} & \mathrm{DCM} \end{cases}$$

$$\text{where } R_{\mathrm{cri}} = \frac{2L_a}{J_{\mathrm{cri}}\,(d_a)\,T_s}. \tag{9}$$

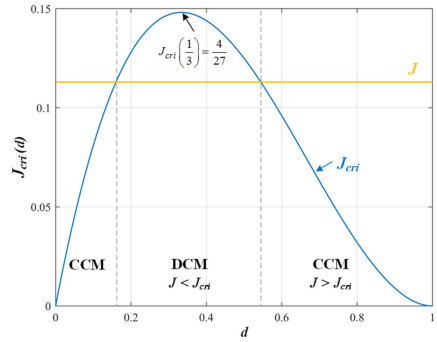

Fig. 4. Function relationship between the boundary-mode criterion and the duty cycle.

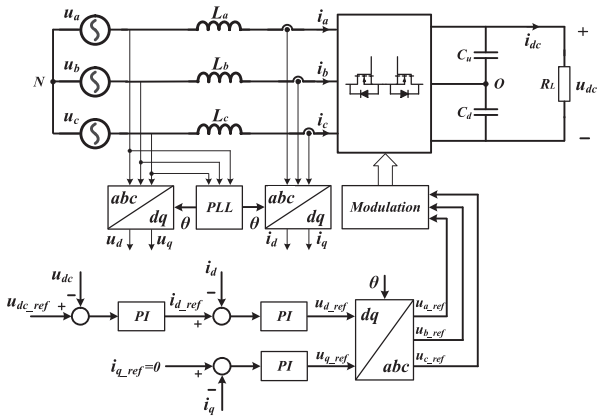

Fig. 5. Typical control strategy for the three-phase Vienna rectifier in a synchronous rotating coordinate system.

$R_{\rm cri}$ is the load value for boundary mode. When $R_L < R_{\rm cri}$, the Vienna operates in CCM. On the contrary, Vienna operates in DCM. The Vienna rectifier entering DCM is a signal of light load since the inductor current is insufficient to maintain continuous conduction at this time. When the inductance and switching frequency are fixed, the minimum critical load value can be calculated. In the steady state, $u_{\rm dc}$ should be controlled to the reference $u_{\rm dc\_ref}$, then the corresponding load current critical value can be obtained

$$i_{\rm light} = \frac{u_{\rm dc\_ref}}{R_{\rm cri}}. \tag{10}$$

The operating state of Vienna is determined according to the above equation. When $i_{\rm dc} > i_{\rm light}$, Vienna is in the normal state. When $i_{\rm dc} < i_{\rm light}$, Vienna is in light-load condition

$$G_{v\_B} = \begin{cases} \frac{1}{1-d_a} & \text{CCM} \\ \frac{1+\sqrt{1+4d_a^2/J}}{2} & \text{DCM.} \end{cases} \tag{11}$$

Generally, DCM can be found in all boost converter-derived topologies. Under light-load conditions, Vienna rectifiers are prone to enter DCM, which is unavoidable. When operating in DCM, the energy stored in the inductor is fully discharged, the inductor current drops to zero during each switching cycle, and the voltage gain differs from that in CCM, as shown in (11). Due to the discontinuity of the current, the system exhibits nonlinear characteristics, and the instantaneous power transfer of the rectifier is unstable, and no energy is transferred to the output during some switching cycles, resulting in unstable output power on the dc side. This fluctuation in power transmission will cause the dc-side voltage to fluctuate more at light loads. On the other hand, Vienna rectifier controller is generally optimized for CCM, while DCM cannot respond quickly and accurately to load changes, and the performance of the feedback control loop at light loads is reduced, making it difficult to maintain a constant output voltage.

III. Vienna Rectifier Direct Modulation Index Control Strategy Under Light Load

A. Normal State Control Strategy

The three-phase Vienna rectifier is a boost-type PFC, so it is also suitable for the control method of the three-phase PWM rectifiers. The typical control strategy in the synchronous rotating coordinate system is shown in Fig. 5. The control strategy includes a voltage outer loop and a current inner loop. The voltage outer loop is employed to control $u_{\rm dc}$ stability, and its output is taken as the reference $i_{d\_\rm ref}$ for the current loop d-axis, which contains the current amplitude information. The current inner loop controls the amplitude and phase of the input current. The q-axis current reference $i_{q\_\rm ref}$ is set to 0 to achieve PFC. The current loop outputs $u_{d\_\rm ref}$ and $u_{q\_\rm ref}$, after dq/abc transformation, are taken as the three-phase voltage reference $u_{x\_\rm ref}$ $(x = a,b,c)$ to generate the modulation signals.

If the influence of the q-axis component is ignored, $u_{d\_\rm ref}$ represents the amplitude of $u_{x\_\rm ref}$. The modulation index of the system is defined as follows:

$$M = \frac{2u_{d\_\rm ref}}{u_{\rm dc}}. \tag{12}$$

The duty cycle d_x of the three-phase switch is calculated based on $u_{x\_\rm ref}$, which can be expressed as follows:

$$\begin{aligned} d_x &= 1 - \frac{|u_{x\_\rm ref}|}{u_{\rm dc}/2} = 1 - \frac{2\,|u_{d\_\rm ref}\sin\omega t_x|}{u_{\rm dc}} \\ &= 1 - M\,|\sin\omega t_x|\,, x = a,b,c. \end{aligned} \tag{13}$$

The modulation index can be directly modified by adjusting $u_{d\_\rm ref}$, thus changing the amplitude of the duty ratio. Taking a-phase as an example, under normal conditions, the duty cycle and drive signal of the Vienna rectifier are shown in Fig. 6(a). At this time, $M<1$, $d_a>0$, and S_a always operates in PWM mode during one line period. If $u_{d\_\rm ref}$ is increased, M is also increased, the amplitude of the duty cycle will increase accordingly, while the average value of the duty cycle decreases. When $M>1$, near the peak of u_a, $d_a = 0$ and S_a is in the OFF-state. At this time, the duty cycle and drive signal are shown in Fig. 6(b). Only near the zero-crossing point of u_a, which is shaded in Fig. 6(b), $d_a>0$, and S_a operates in PWM mode. At light loads, high M ensures that the duty cycle is 0 for most of the time, thereby reducing energy transfer.

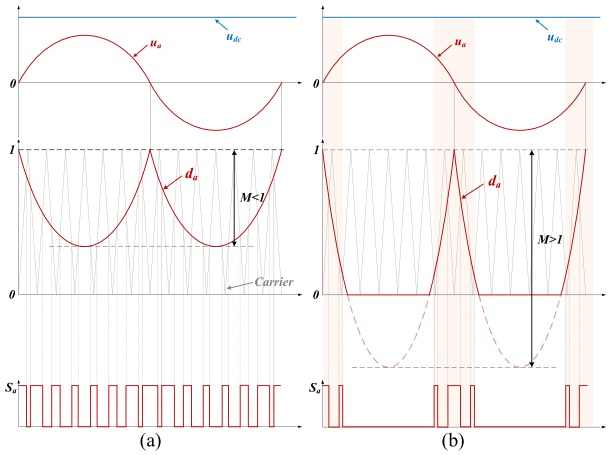

Fig. 6. Duty cycle and drive signal under different modulation indices. (a) Modulation index less than 1. (b) Modulation index greater than 1.

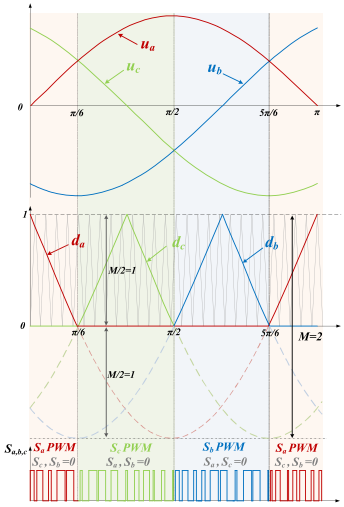

Fig. 7. Three-phase duty cycle and switching state when the modulation index is equal to 2.

B. Proposed Light-Load Control Strategy Based on the Modulation Index

Vienna rectifiers can only transfer energy unidirectionally. For control systems based on the *dq* rotating coordinate system, when operating under no load, if the control method, as shown in Fig. 5, is still employed, the u_{d_ref} calculated by the PI controller will exceed the theoretical steady-state value and continue increasing, to further reduce the conduction time of the switches, which will ultimately lead to dc-side overvoltage.

As seen from the previous analysis, the rectifier will transfer energy to the dc side as long as a switch is turned ON. To reduce the transfer power, it is essential to minimize the switch-ON time. At light loads, it is possible to consider directly controlling the modulation index to change the duty cycle. According to the trigonometric function relationship and (12), when $u_{d\_\mathrm{ref}} \geq u_{\mathrm{dc}}$, $M \geq 2$, there is no overlap in the conduction time of the three-phase switches, as shown in Fig. 7. It can be seen that d_a decreases to 0 at $\pi/6$ and increases from 0 at $5\pi/6$. In the interval $[\pi/6, 5\pi/6]$, $d_a = 0$, $S_a = 0$, and the a-phase switching devices

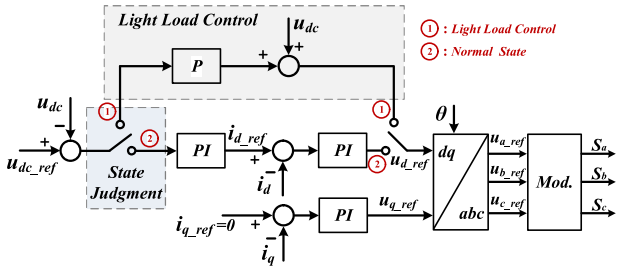

Fig. 8. Control block diagram of the proposed direct modulation index control strategy under light load.

always remain OFF. Only in the intervals $[0, \pi/6]$ and $[5\pi/6, \pi]$, S_a operates in PWM mode, while S_b and S_c remain OFF. In this case, at most, only one phase switch is in PWM mode at any time, while the other two are turned OFF. Therefore, at any given time, energy is transferred to the dc side through only one phase at most, the average duty cycle is effectively decreased, and the energy obtained from the ac side is greatly reduced. For no-load conditions, most of the time, all switching devices are turned OFF. When any one of the switches is turned ON, the three-phase system does not form a current loop so that no energy is transferred to the dc side.

At light loads, there is almost no energy consumption on the dc side, the load power demand is significantly reduced, and the rectifier operates at DCM, but the power conversion process continues. The system has less inertia and is more sensitive to disturbances. The accuracy and sensitivity of the PI controller are not sufficient to provide a fast dynamic response. The voltage loop may undergo frequent adjustments, while the response time and feedback loop of the current loop experience a certain delay. In addition, the optimal parameters for the PI controller are different under light-load and normal state. The PI controller parameters are generally optimized for heavy-load conditions. Under normal conditions, the current loop can respond quickly and accurately to load changes to ensure stable u_{dc}. However, at light loads, the feedback signal in the current loop is small, and its regulation capability is greatly weakened. The system tries to regulate the u_{dc} to remain stable, but the integral term is prone to over-reaction, causing the PI controller to constantly correct the calculated values of u_{d_ref} and i_{d_ref}. The end result is fluctuations in u_{dc}. At light load, the proportional and integral parameters should be reduced to avoid voltage oscillations caused by overshoot and excessive response. The operating parameters of the PI controller can be dynamically modified according to the system load conditions, but parameter tuning is complex [23].

Fig. 8 shows the control block diagram of the proposed light-load control strategy, which is implemented with *P* control and dc-side voltage feedforward. *P* control monitors the u_{dc} in real time and amplifies the error between u_{dc} and $u_{\mathrm{dc\_ref}}$. At light loads, the u_{dc} changes relatively slowly and a small steady-state error is allowed, which will not significantly affect the system performance. Although PI control can eliminate the steady-state error, it may introduce unnecessary delay and overshoot at light loads. The integral term accumulates error, which may cause the system to overreact, resulting in voltage fluctuations and

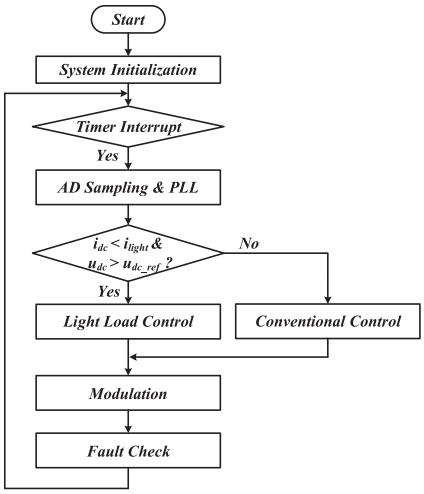

Fig. 9. Algorithm flowchart of the proposed light-load control strategy.

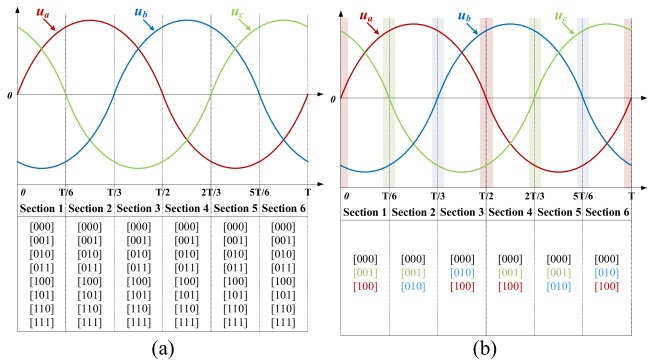

Fig. 10. Six operating sections and switching state distribution of the Vienna rectifier. (a) Normal state. (b) At light load.

oscillations. Therefore, a *P* controller can provide fast response characteristics and is easier to implement than a PI controller. Under light-load conditions, even if a certain steady-state error may be introduced by *P* control, it is acceptable as long as $u_{\rm dc}$ is stable. In addition, since $u_{d\_\rm ref} > u_{\rm dc}$ can ensure that, at most, one phase switch is turned ON at any time, $u_{\rm dc}$ can be employed as a feedforward component, which is added with *P* control output to form $u_{d\_\rm ref}$. In this way, the response can be further accelerated, and corrections can be made immediately once a load step occurs.

The algorithm flowchart of the proposed light-load control strategy is shown in Fig. 9. First, the operating state of Vienna is determined based on the analysis in Section II. The state judgment depends on two key parameters: $i_{\rm dc}$ and $u_{\rm dc}$. $i_{\rm dc}$ is the most direct parameter for judging the light-load condition. $u_{\rm dc}$ is employed to detect overvoltage. When switching to a light load, the system suffers from power imbalance, and the energy stored on the dc side cannot be consumed in time, which causes $u_{\rm dc}$ to increase. Relying on only one parameter alone may make it more prone to state misjudgment due to errors. Moreover, the mean value filtering method, digital, and analog filters are adopted to eliminate noise and errors, ensuring the accuracy of the sampling signals. Therefore, to ensure the reliability of state judgment, the criterion for light-load conditions can be summarized as $i_{\rm dc} < i_{\rm light}$ and $u_{\rm dc} > u_{\rm dc\_ref}$. Then, when the system enters light-load mode, the control strategy, as shown in Fig. 8, is adopted. Under normal conditions, the typical control strategy, as shown in Fig. 5, is adopted. After state judgment, when operating in light-load control, the switch position is 1, and the sum of *P* control and dc voltage feedforward is adopted as the $u_{d\_\rm ref}$. When operating in the normal state, the switch position is 2, and the output of the PI current loop control is adopted as the $u_{d\_\rm ref}$. The two states correspond to two different control methods, and the $u_{d\_\rm ref}$ value is one or the other.

C. Operating Principle of the Proposed Light-Load Control

According to the polarity of each phase voltage, one line period can be divided into six sections with a 60° interval, as shown in Fig. 10(a). For the normal state, S_x always works in PWM mode, and each section contains eight operating modes [S_a S_b S_c], as shown in the table in Fig. 10(a). Among them, "1" represents that the switch of this phase is turned ON, and "0" represents that the switch is turned OFF. Take section 2 as an example (u_a>0, u_b<0, and u_c<0). Fig. 11 shows the operating modes and current loops under different switching states.

For the proposed light-load control strategy, when *M* is large enough, S_x only operates in PWM mode near the zero-crossing point of u_x. In the interval [*T*/6, *T*/4], S_c operates in PWM mode, and there are only two energy transfer paths ([000] and [001]). In the interval [*T*/4, *T*/3], S_b operates in PWM mode, and there are also only two energy transfer paths ([000] and [010]). The original eight operating modes in section 2 are simplified to three, that is, [0 0 0], [0 0 1], and [0 1 0], as shown in Figs. 10(b) and 11. Most of the time, all switches are turned OFF and the switching state is [0 0 0], with almost no power flowing. At any given time, at most, one phase switch is in PWM mode so that energy transfer is limited to a certain phase. As a result, the energy transfer paths can be reduced, which simplifies the operating principle and control strategy at light loads.

D. Stability Analysis

Since the *q*-axis current is employed to achieve PFC in the three-phase Vienna rectifier, whose reference is 0, it does not affect the stability of the *d*-axis. Therefore, the main dynamic characteristics of the system can be determined by analyzing the transfer function of the *d*-axis.

When the system satisfies the unity power factor, the control block diagram of the normal-mode control strategy can be simplified, as shown in Fig. 12(a), where $G_v(s)$ is the voltage loop PI controller, $C_{\rm dc}$ is the dc-side capacitor, and i_c is the capacitor current. The open-loop transfer function of the traditional control strategy can be obtained as follows:

$$G_{v\_\rm open} = G_v(s)\, G_{i\_\rm close}(s)\, \frac{3u_d}{2u_{\rm dc}} \frac{R_L}{sR_L C_{\rm dc} + 1} \tag{14}$$

where $G_{i\_\rm close}(s)$ represents the current loop closed-loop transfer function, which can be expressed as follows:

$$G_{i\_\rm close} = \frac{G_i(s)\, K_P}{(0.5T_s s + 1)(sL_a + R) + G_i(s)\, K_P} \tag{15}$$

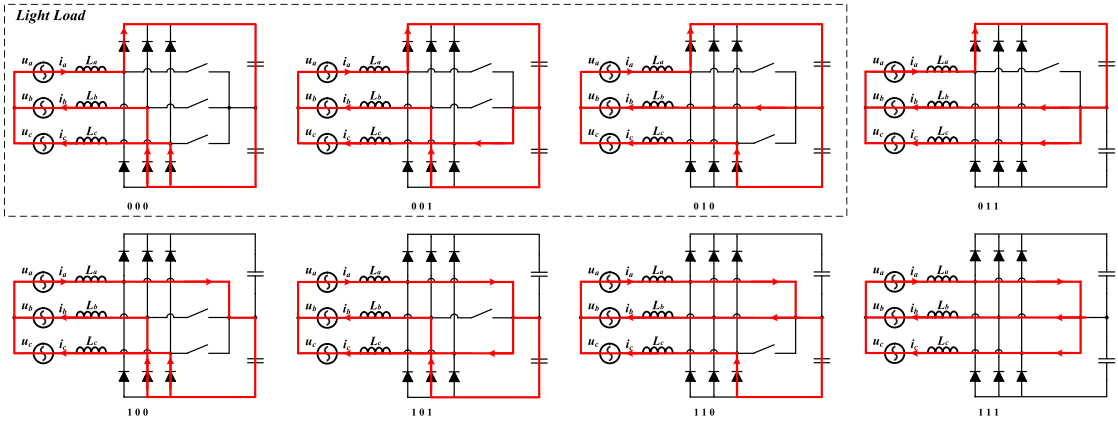

Fig. 11. Operating modes and current loops under different switching states [S_a S_b S_c] in section 2.

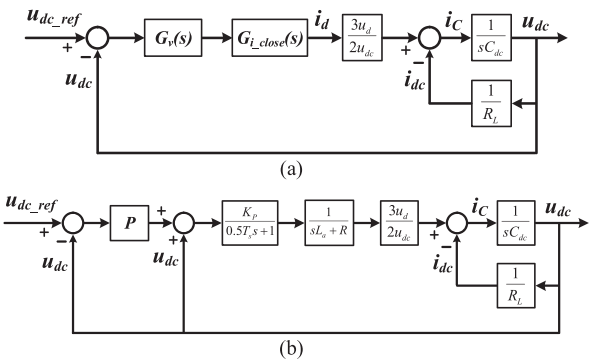

Fig. 12. Simplified control block diagram of the (a) traditional control strategy and (b) proposed control strategy.

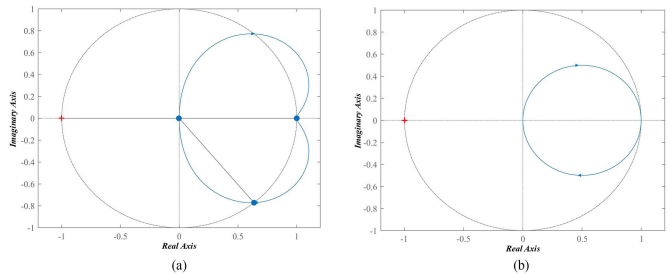

Fig. 13. Nyquist diagram of the (a) traditional control strategy under heavy load and (b) proposed control strategy under light load.

where $G_i(s)$ represents the current loop PI controller, K_P is the PWM gain, T_s is the sampling period, and R is the inductance resistance. Fig. 13(a) shows the Nyquist diagrams of the normal-mode control strategy.

The proposed light-load direct modulation index control strategy employs P control instead of the voltage and current double-loop PI control, and its simplified control block diagram is shown in Fig. 12(b). The open-loop transfer function of the proposed strategy can be expressed as follows:

$$G_{p\_\text{open}} = \frac{3u_d P K_P R_L}{2u_{\text{dc}}\left(0.5T_s s+1\right)\left(sL_a+R\right)\left(sR_L C_{\text{dc}}+1\right)}. \quad (16)$$

The Nyquist diagram of the proposed strategy is shown in Fig. 13(b). The Nyquist curves of both the traditional control under heavy load and the proposed strategy under light load do not enclose the point $(-1, j0)$ and do not introduce unstable poles in the right half plane. It can be concluded that the proposed strategy is stable.

IV. Simulation and Experiment

A. Simulation Verification

The Vienna rectifier model is built in PSIM for simulation. Fig. 14(a) and (b) shows the simulation waveforms of no and light loads without the proposed direct modulation index control strategy, respectively. It can be seen that, at no load, the u_{d_ref} calculated according to the double-closed-loop control will exceed the theoretical steady-state value and continue increasing to reduce the switch-ON time, which will eventually result in an overvoltage of the u_{dc}. At this time, with the traditional control strategy, the amplitude of the duty cycle is slightly greater than 1, and most of the time, S_x in one line period is in PWM mode.

For light-load mode, the energy stored on the dc side cannot be consumed in time, while the response speed and regulation capability of the PI controller are insufficient. The current loop cannot provide the accurate response, so the integral of the PI controller in the voltage loop is prone to over-reaction. i_{d_ref} constantly adjusts to control the power supply of the grid current, causing u_{dc} to oscillate. u_{d_ref} cannot achieve high-precision output, and u_{dc} fluctuates widely, which is not conducive to the stable operation of the rectifier.

Fig. 15 shows the simulation waveform of the proposed control strategy. When the Vienna load changes, u_{dc} can be stably controlled with almost no fluctuation. Since the modulation index is directly adjusted by adjusting the amplitude of u_{d_ref}, the proposed strategy can provide excellent dynamic response and nearly no voltage overshoot during no-load switching. In steady state, different control strategies are adopted for the two load conditions. At light load, M>2, the amplitude of the duty cycle is much larger than that in normal mode. Only one phase switch is in PWM mode at most, which can effectively limit energy transfer.

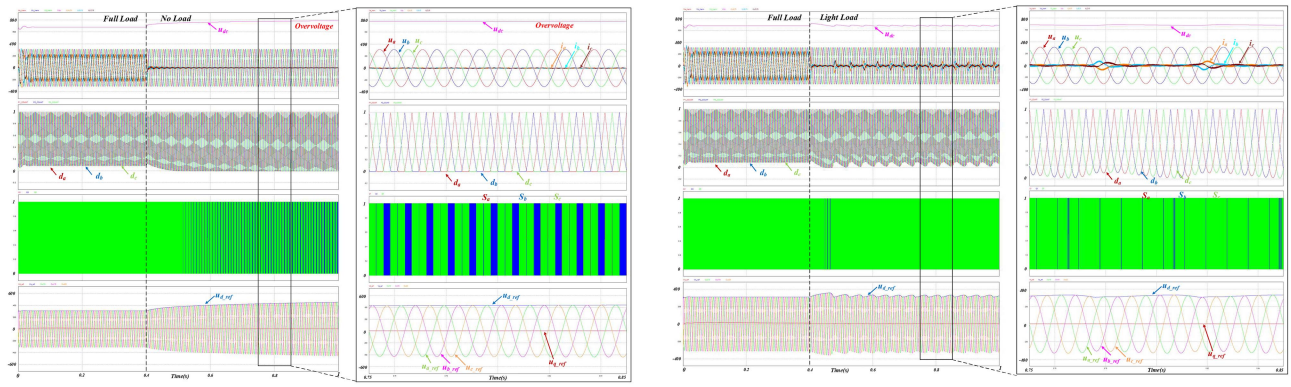

(a) (b)

Fig. 14. Simulation waveforms without the proposed direct modulation index control strategy. (a) At no load. (b) At light load.

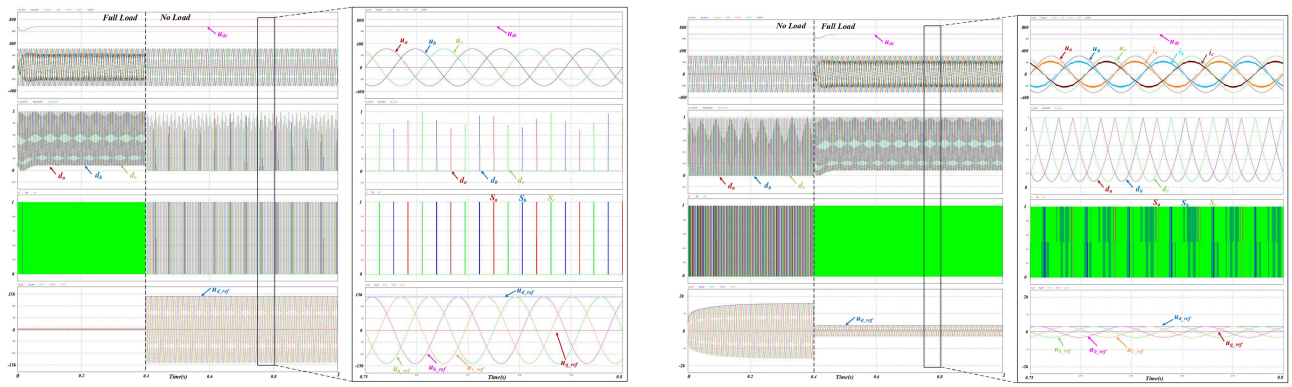

(a) (b)

Fig. 15. Simulation waveforms with the proposed control strategy. (a) Normal condition switching to no load. (b) No load switching to normal condition.

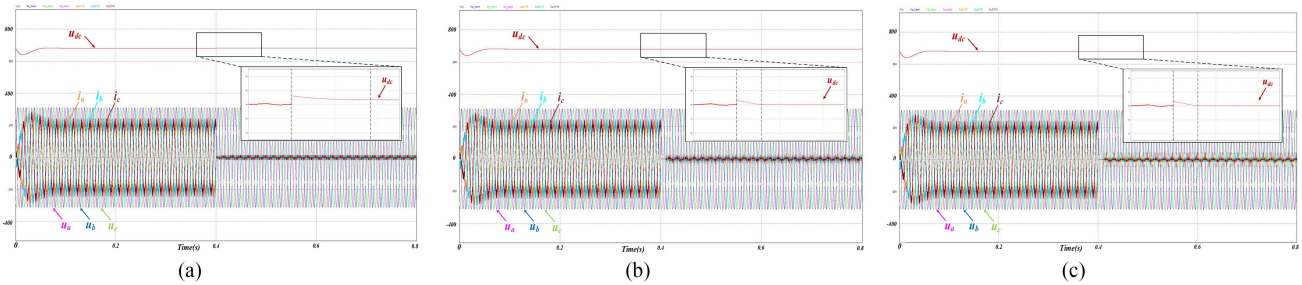

(a) (b) (c)

Fig. 16. Control effect when switching from normal-mode to 100-W light-load condition using different proportional gains. (a) P=300. (b) P=6000. (c) P=30 000.

Fig. 16 verifies the control effect when switching from normal mode to 100-W light-load condition using different proportional gains. It can be seen that different proportional gains can ensure the stability of u_{dc} under light load. A lower proportional gain ($P = 300$) results in a slower voltage response, and voltage deviations may occur when the load changes. A higher proportional gain (when $P = 6000$) can improve the response speed. However, when the proportional gain is further increased (when $P = 30\ 000$), there will be no significant improvement in the dynamic response, which may lead to high spikes in the ac current. The proportional gain selected in this article is 6000, which balances response speed and stability.

B. Experimental Verification

To verify the feasibility of the proposed strategy, a 50-kW three-phase Vienna rectifier prototype is designed and built. The prototype is shown in Fig. 17, and the system specifications

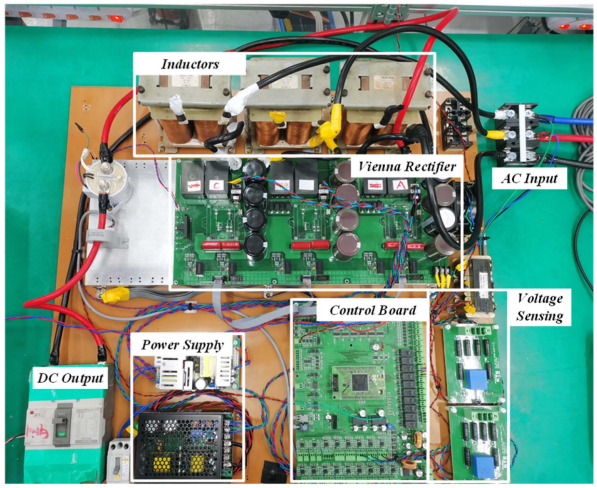

Fig. 17. Designed three-phase Vienna rectifier prototype.

TABLE I
PROTOTYPE SPECIFICATIONS

Parameter	Value
Single-phase AC Input RMS Voltage	220 V
DC Output Reference Voltage	600 V
MOSFET Switching Frequency	24 kHz
Maximum Output Power	50 kW
DC side capacitance	2040 μF
Inductance $L_{a,b,c}$	400 μH
VIENNA Power Module	NXH020U90MNF2PTG

are listed in Table I. The NXH020U90MNF2 is employed as a Vienna power module. The DSP TMS320F28377D is employed as the main controller.

Fig. 18(a)–(c) shows the start-up, 15-kW, and 40-kW steady-state waveforms, respectively, under normal states. In the normal state, a double-loop control strategy in the *dq* coordinate system, as shown in Fig. 5, is adopted. The system provides good dynamic and steady-state responses. Except for light-load conditions, the total harmonic distortion (THD) is less than 5%, with a minimum THD of 2.5%, and the efficiency is higher than 98%, with a maximum efficiency of 99.23%.

The dynamic experimental waveforms of the 1.2-kW light load without and with the proposed control strategy are shown in Fig. 19(a) and (b), respectively. The steady-state experimental waveforms of the 1.2-kW light load without and with the proposed control strategy are shown in Fig. 20(a) and (b), respectively. For the traditional strategy, the same control strategy is adopted as in the normal state. As can be seen, similar to the simulation results, the $u_{\rm dc}$ contains a ripple of nearly 50 V at light load, and the ac-side input current fluctuates accordingly, which is detrimental to system safety and stability. Therefore, the normal state control strategy, as shown in Fig. 5, is not applicable under light load. In contrast, for the proposed direct modulation index control strategy, when switching to light load, $u_{\rm dc}$ has very little overshoot and responds quickly. At light-load steady state, $u_{\rm dc}$ contains almost no ripple.

The dynamic experimental waveforms of the 720-W light load without and with the proposed control strategy are shown in Fig. 21(a) and (b), respectively. When the traditional method is adopted, $u_{\rm dc}$ will rapidly increase to trigger overvoltage protection at the moment of load switching. For lighter loads, the overvoltage protection will also be triggered, which is not beneficial to the safe operation of the system. Therefore, the traditional strategy is not feasible under such very light loads and no loads. Instead, the proposed strategy ensures smooth switching to light-load mode with almost no voltage fluctuation.

Figs. 22–24 show the experimental waveforms at 150 W, 100 W, and no load, respectively, with the proposed direct modulation index control strategy. Under different light-load conditions, the proposed strategy can quickly respond to light-load changes, and the $u_{\rm dc}$ in the transient state also fluctuates very little. In steady state, the proposed strategy can achieve stable control of $u_{\rm dc}$ under all conditions, and the ripple content is very low compared with the traditional method. As can be seen from the steady-state waveform, the proposed strategy cannot achieve PFC and low THD under light load, and the current has high spikes, but this will not cause system failure. The current waveform exhibits the characteristics of a "tall and skinny" shape, which is similar to the diode uncontrolled rectification waveform. At light loads, a tradeoff is required between the $u_{\rm dc}$ stability and the ac quality. The $u_{\rm dc}$ fluctuation may lead to the degradation of performance and reliability. In particular, under no-load and very light conditions, the proposed strategy can also control the dc voltage to remain stable without triggering overvoltage protection, which is not provided by other methods. Under such light-load conditions, the current THD will not be ideal no matter which control method is adopted.

Fig. 25 shows the transient response waveform when the system switches between 7.2 kW and 100 W with the proposed strategy. The proposed strategy not only responds to light-load changes but also maintains excellent voltage stability during high-power load step. The low oscillation of both $u_{\rm dc}$ and i_a verifies that the proposed strategy can ensure that the system quickly and stably returns to normal mode. In addition to the switching between light-load and normal mode, Fig. 26 shows the dynamic waveform when the light-load condition changes between 820 and 100 W. When the system switches between different light-load conditions, the $u_{\rm dc}$ also fluctuates very little, indicating that the proposed strategy offers good steady-state regulation performance under light-load conditions as well. The above experimental results further demonstrate that the proposed approach can provide stability and fast dynamic response when switching across the full-load range.

At light loads, the efficiency measurement may not be very stable and accurate. This is because the ac-side current always fluctuates and has spikes, resulting in unstable current measurements. It is essential to highlight that, although the proposed strategy efficiency, PF, and THD are limited at light loads, it ensures system stability and reliability under conditions where the traditional strategy fails. If the system stability cannot be guaranteed, then there is no meaning in discussing efficiency and THD. During light-load conditions, the power drawn from the grid is low, so a low THD and efficiency will not have a

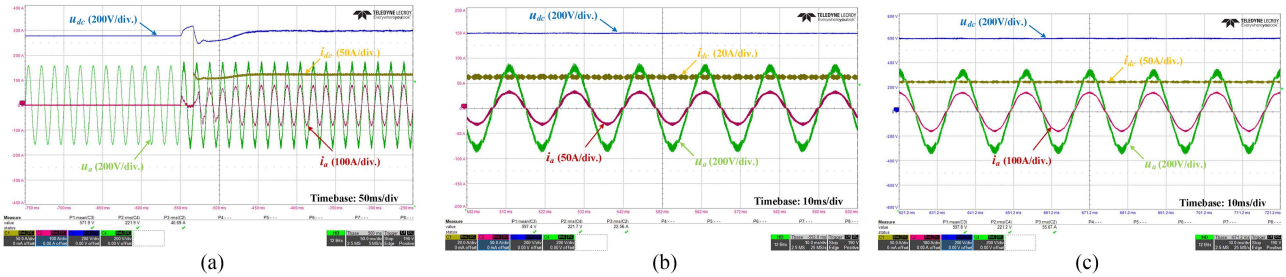

(a) (b) (c)

Fig. 18. Experimental waveforms under normal condition. (a) Start-up. (b) 15-kW steady state. (c) 40-kW steady state.

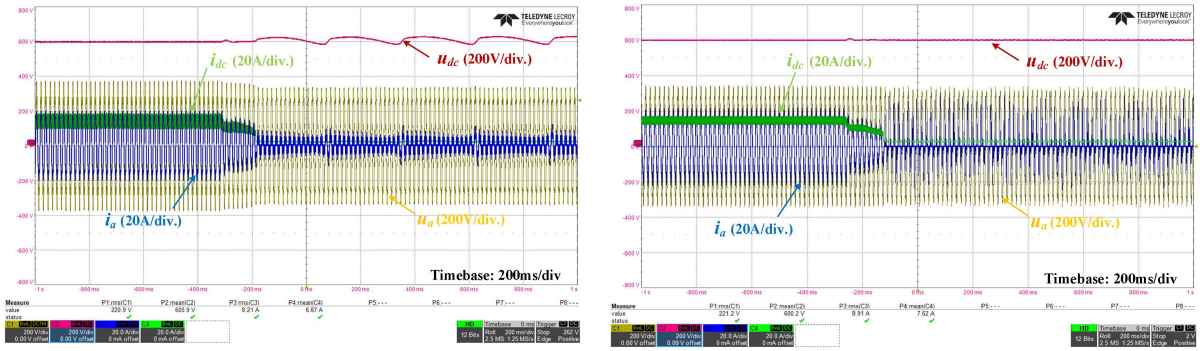

(a) (b)

Fig. 19. Experimental dynamic waveforms when switching to 1.2-kW light-load conditions. (a) Traditional strategy. (b) Proposed strategy.

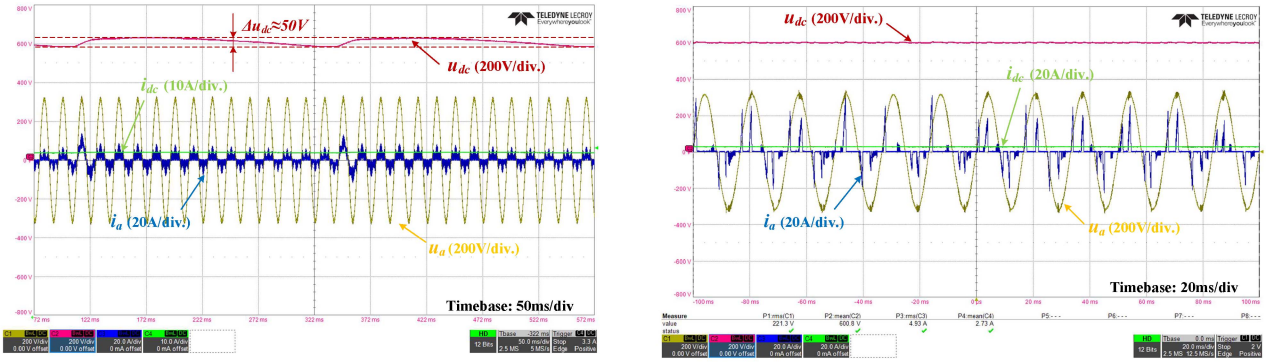

(a) (b)

Fig. 20. Experimental steady-state waveforms under 1.2-kW light-load conditions. (a) Traditional strategy. (b) Proposed strategy.

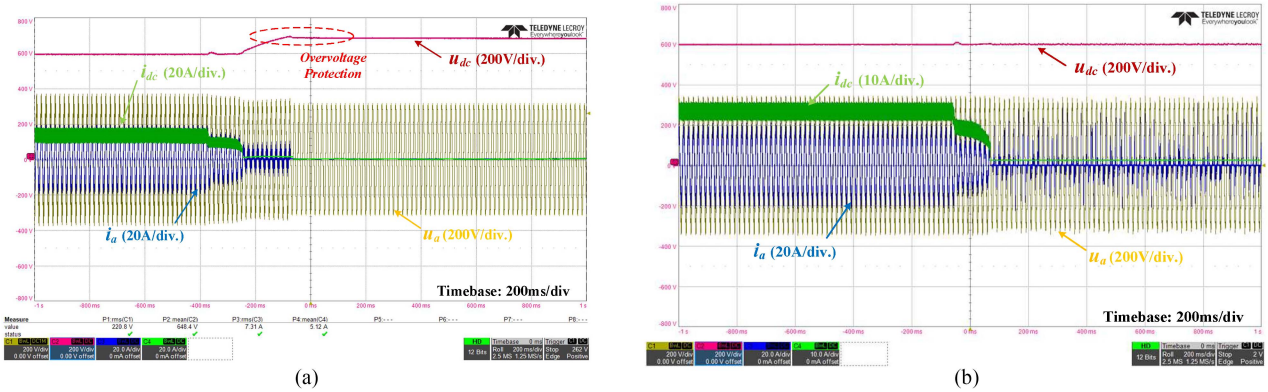

(a) (b)

Fig. 21. Experimental dynamic waveforms when switching to 720-W light-load conditions. (a) Traditional strategy. (b) Proposed strategy.

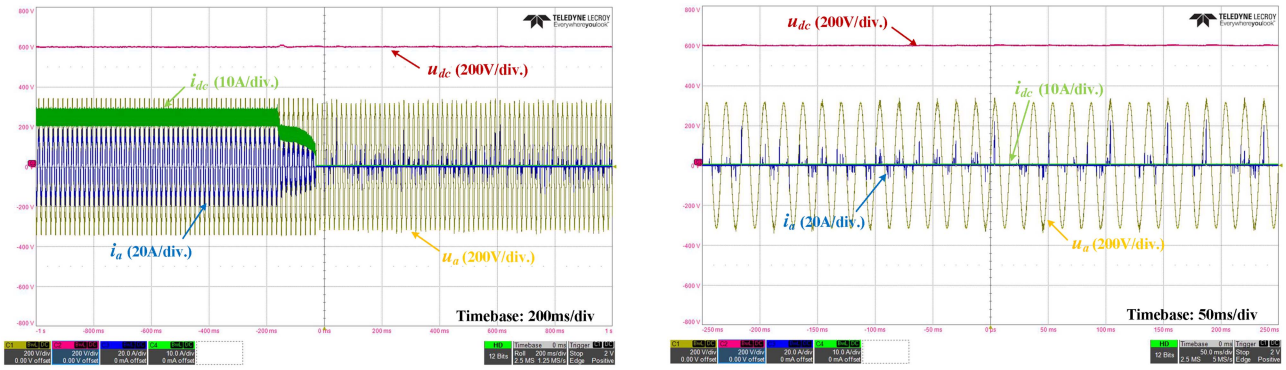

(a) (b)

Fig. 22. Experimental waveforms of 150-W light load with the proposed strategy. (a) Dynamic. (b) Steady state.

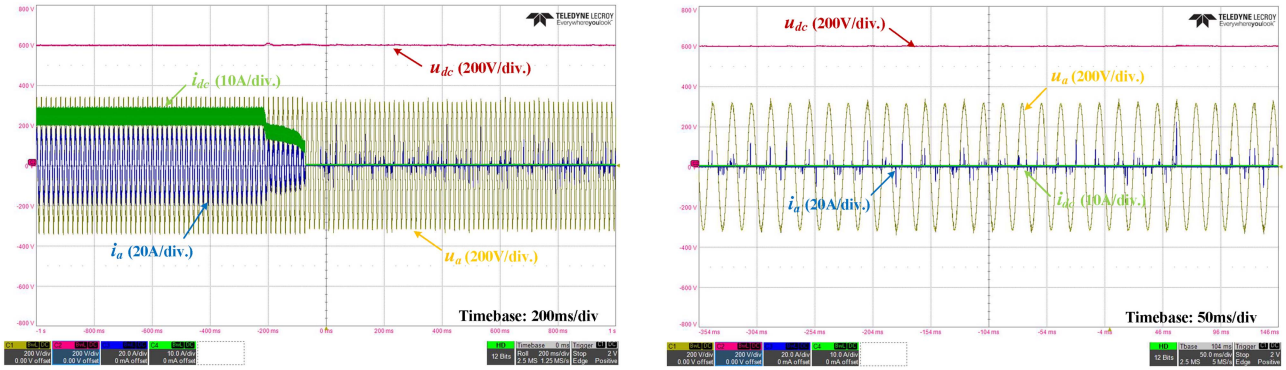

(a) (b)

Fig. 23. Experimental waveforms of 100-W light load with the proposed strategy. (a) Dynamic. (b) Steady state.

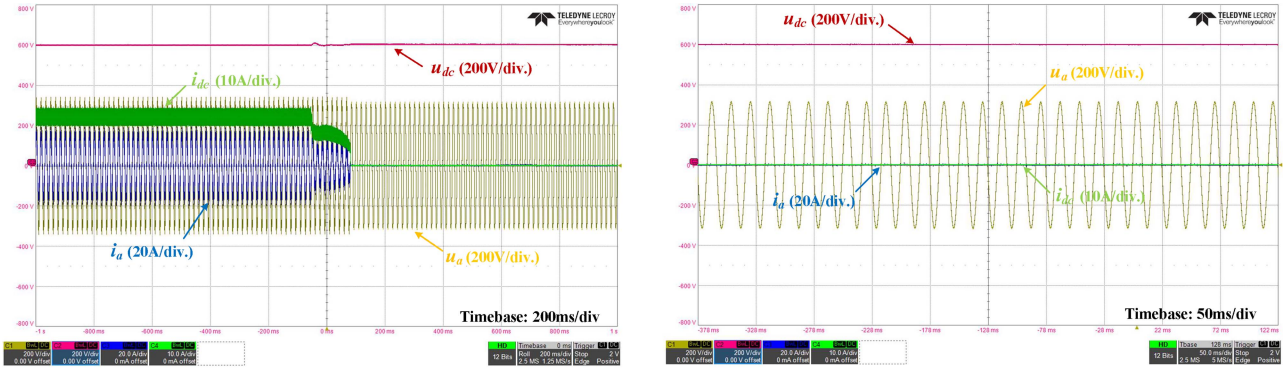

(a) (b)

Fig. 24. Experimental waveforms of no load with the proposed strategy. (a) Dynamic. (b) Steady state.

significant impact on grid stability. The efficiency and power quality issues should be focused more on rated load and high power, therefore ensuring reliable operation under light loads more than efficiency and power quality improvement.

Table II compares the proposed strategy with previous works. Compared with previous works, the proposed method provides better dc voltage stability and dynamic response. However, the price is that THD and power factor (PF) are not excellent. In the proposed method, due to the uneven switching distribution at light loads, the input current deviates from the ideal sine wave, and the high spikes result in high THD and low PF. However, in normal mode, the fundamental current increases, the input current becomes more sinusoidal, the relative percentage of harmonics decreases, and the PF tends to increase. The proposed strategy was tested under more comprehensive light-load conditions. The proposed control strategy is entirely software-based, without modifying the hardware circuit, so it is easy to apply or extend to other Vienna rectifiers. In summary, the

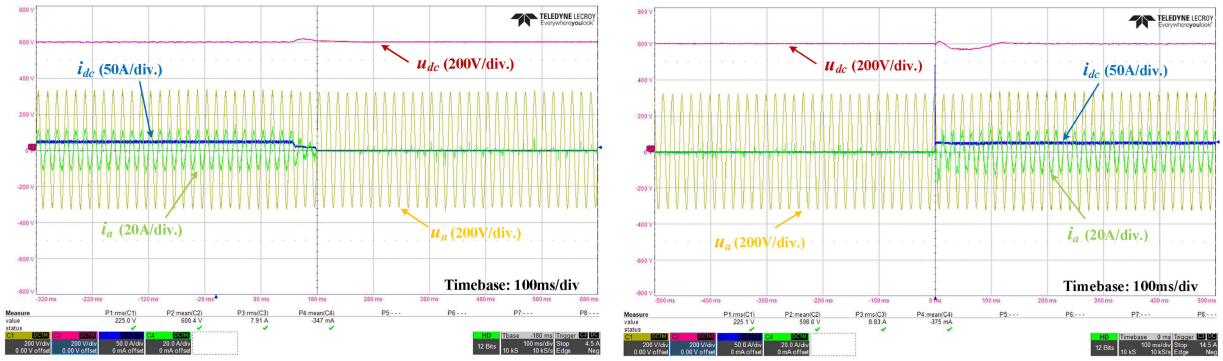

Fig. 25. Transient response waveform when the system switches between 7.2 kW and 100 W with the proposed strategy. (a) 7.2 kW–100 W. (b) 100 W–7.2 kW.

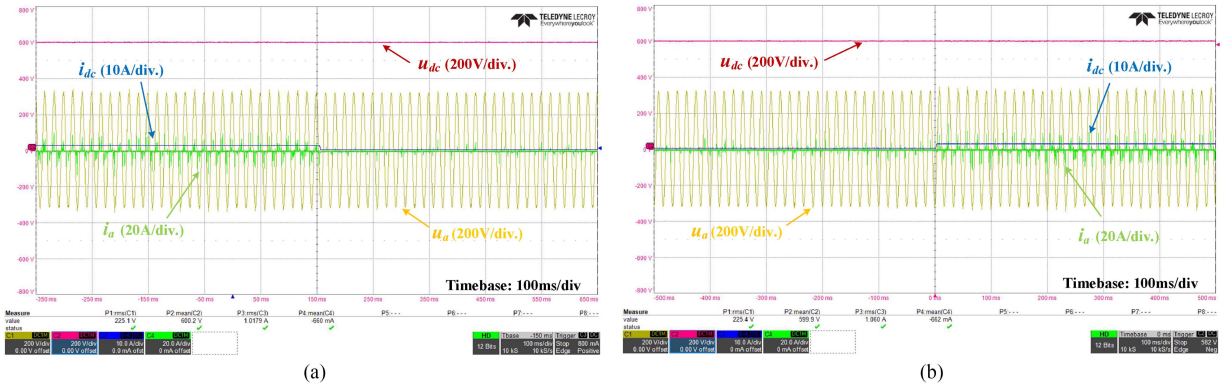

Fig. 26. Dynamic waveform when the light-load condition changes between 820 and 100 W. (a) 820–100 W. (b) 100–820 W.

TABLE II
COMPARISON OF THE PROPOSED METHOD WITH PREVIOUS WORKS

	Light load power	DC voltage ripple rate	Overshoot	Transient time	THD	PF
Proposed	1.2 kW	<0.25%	≤1.7%	<150 ms	>150%	0.53
	100 W	<0.15%	≤1.7%	<150 ms	>100%	0.62
	No load	<0.1%	≤1.7%	<150 ms	-	-
Traditional	1.2 kW	8.33%	6%	>330 ms	>65%	0.8
	<720 W	Overvoltage	-	-	-	-
	No load	Overvoltage	-	-	-	-
[7]	No load	Unknown	>5.6%	Unknown	-	-
[13]	No load	0.25%	>6%	Unknown	-	-
[16]	100 W (Simulation)	Unknown	1.1%	>120 ms	Unknown	Unknown
[21]	320 W	>2.6%	Unknown	Unknown	>44.1%	Unknown

proposed direct modulation index control strategy can provide excellent dynamic and steady-state responses at light loads, thereby optimizing the light-load performance and stability of the Vienna rectifier.

V. CONCLUSION

This article proposes a direct modulation index control strategy to mitigate u_{dc} fluctuations under light load. First, the single-phase Vienna rectifier is modeled as a boost converter. Based on this, the critical load current value of the transition from CCM to DCM is analyzed, and a light-load state judgment criterion is obtained. Then, under the synchronous rotating reference frame control strategy, the effect of the modulation index on the duty cycle and drive signal is discussed. When the modulation index exceeds 2, there is no overlap in the conduction time of the three-phase switches, and at any time, only one phase switch is in PWM mode at most, so the energy obtained from the ac side is greatly reduced. By adjusting the modulation index, the duty cycle can be greatly reduced. Therefore, a direct modulation index light-load control strategy is proposed, which is implemented using proportional control and voltage feedforward.

Moreover, the proposed control strategy is adopted at light load, while under normal conditions, the conventional control strategy is still adopted. The proposed strategy simplifies the original eight operating modes to three, which reduces the energy transfer path and simplifies the operating principle. Finally, to validate the effectiveness of the proposed strategy, a 50-kW three-phase Vienna rectifier prototype is designed and built. Simulation and experimental results show that under different light-load conditions, the proposed strategy can quickly respond to light-load changes, and there are minimal u_{dc} fluctuations in the transition. Stable u_{dc} control is also achieved in steady-state operation. In the future, the following two aspects can be considered for in-depth research of the light-load control strategy. One is to improve the current THD and PFC under light-load conditions while ensuring the stability of the u_{dc}. The second is to explore the segmented optimization control strategy under different load conditions.

References

[1] J.-S. Lee and K.-B. Lee, "Predictive control of Vienna rectifiers for PMSG systems," *IEEE Trans. Ind. Electron.*, vol. 64, no. 4, pp. 2580–2591, Apr. 2017, doi: 10.1109/TIE.2016.2644599.

[2] M.-S. Kim, S.-H. Lee, T.-V. Le, H.-U. Go, S.-J. Park, and Y. Wang, "Harmonic current suppression strategy for the VIENNA rectifier based on discrete Fourier transform," *IEEE J. Emerg. Sel. Topics Power Electron.*, vol. 13, no. 2, pp. 2307–2318, Apr. 2025, doi: 10.1109/JESTPE.2025.3532681.

[3] A. R. Izadinia and H. R. Karshenas, "Current shaping in a hybrid 12-pulse rectifier using a Vienna rectifier," *IEEE Trans. Power Electron.*, vol. 33, no. 2, pp. 1135–1142, Feb. 2018, doi: 10.1109/TPEL.2017.2685459.

[4] M. Zhang, Y. Yuan, X. Sun, Y. Zhang, and X. Li, "Harmonic resonance suppression strategy of the front-end Vienna rectifier in EV charging piles," *IEEE Trans. Power Electron.*, vol. 38, no. 1, pp. 1036–1053, Jan. 2023, doi: 10.1109/TPEL.2022.3204537.

[5] J.-S. Lee and K.-B. Lee, "A novel carrier-based PWM method for Vienna rectifier with a variable power factor," *IEEE Trans. Ind. Electron.*, vol. 63, no. 1, pp. 3–12, Jan. 2016, doi: 10.1109/TIE.2015.2464293.

[6] J.-S. Lee and K.-B. Lee, "Carrier-based discontinuous PWM method for Vienna rectifiers," *IEEE Trans. Power Electron.*, vol. 30, no. 6, pp. 2896–2900, Jun. 2015, doi: 10.1109/TPEL.2014.2365014.

[7] M. Leibl, J. W. Kolar, and J. Deuringer, "Sinusoidal input current discontinuous conduction mode control of the Vienna rectifier," *IEEE Trans. Power Electron.*, vol. 32, no. 11, pp. 8800–8812, Nov. 2017, doi: 10.1109/TPEL.2016.2641502.

[8] J. Wang, S. Feng, and F. Kurokawa, "Analog controlled critical conduction mode three-phase Vienna rectifier," *IEEE Trans. Ind. Appl.*, vol. 59, no. 5, pp. 6012–6024, Sep./Oct. 2023, doi: 10.1109/TIA.2023.3275939.

[9] Y. Li et al., "Optimal synergetic operation and experimental evaluation of an ultracompact GaN-based three-phase 10-kW EV charger," *IEEE Trans. Transp. Electrific.*, vol. 10, no. 2, pp. 2377–2396, Jun. 2024, doi: 10.1109/TTE.2023.3297502.

[10] D. Zhang, C. Leontaris, J. Huber, and J. W. Kolar, "Optimal synergetic control of three-phase/level boost–buck voltage DC-link AC/DC converter for very-wide output voltage range high-efficiency EV charger," *IEEE J. Emerg. Sel. Topics Power Electron.*, vol. 12, no. 1, pp. 28–42, Feb. 2024, doi: 10.1109/JESTPE.2023.3300693.

[11] A. Blinov, D. Zinchenko, J. Rąbkowski, G. Wrona, and D. Vinnikov, "Quasi single-stage three-phase filterless converter for EV charging applications," *IEEE Open J. Power Electron.*, vol. 3, pp. 51–60, 2022, doi: 10.1109/OJPEL.2021.3134460.

[12] W. Ding, C. Zhang, F. Gao, B. Duan, and H. Qiu, "A zero-sequence component injection modulation method with compensation for current harmonic mitigation of a Vienna rectifier," *IEEE Trans. Power Electron.*, vol. 34, no. 1, pp. 801–814, Jan. 2019, doi: 10.1109/TPEL.2018.2812810.

[13] X. Tang, Y. Cao, Y. Xing, H. Hu, and L. Xu, "An improved burst-mode control for Vienna rectifiers to mitigate DC voltage ripples at light load," in *Proc. IEEE Appl. Power Electron. Conf. Expo.*, 2018, pp. 1294–1298, doi: 10.1109/APEC.2018.8341183.

[14] C. Ji et al., "Dual-loop control for three-phase Vienna rectifier with duty-ratio feedforward," in *Proc. 45th Annu. Conf. IEEE Ind. Electron. Soc.*, 2019, pp. 1715–1720, doi: 10.1109/IECON.2019.8926674.

[15] M. Darnet, E. Godoy, C. Karimi, and S. Gautrais, "Input currents DCM modelling of a Vienna-based rectifier," in *Proc. IEEE Conf. Control Technol. Appl.*, 2021, pp. 589–594, doi: 10.1109/CCTA48906.2021.9659229.

[16] P. Ide, F. Schafmeister, N. Frohleke, and H. Grotstollen, "Enhanced control scheme for three-phase three-level rectifiers at partial load," *IEEE Trans. Ind. Electron.*, vol. 52, no. 3, pp. 719–726, Jun. 2005.

[17] M. Biason, R. Petrella, S. Calligaro, M. Morandin, and M. Zordan, "Full power range seamless control of three-phase unidirectional Vienna rectifier including partial DCM/CCM operation with low harmonic current distortion even under highly distorted grid," in *Proc. IEEE Energy Convers. Congr. Expo.*, 2020, pp. 2204–2211, doi: 10.1109/ECCE44975.2020.9235343.

[18] M. Leibl, J. W. Kolar, and J. Deuringer, "New current control scheme for the Vienna rectifier in discontinuous conduction mode," in *Proc. IEEE Energy Convers. Congr. Expo.*, 2014, pp. 1240–1247, doi: 10.1109/ECCE.2014.6953543.

[19] Y.-S. Lai and Z.-J. Su, "New integrated control technique for two-stage server power to improve efficiency under the light-load condition," *IEEE Trans. Ind. Electron.*, vol. 62, no. 11, pp. 6944–6954, Nov. 2015, doi: 10.1109/TIE.2015.2436872.

[20] J. Chen, L. Zhang, Z. Chen, X. Gao, Y. Xing, and N. Wu, "A variable feedback control for single phase Vienna rectifiers at non-load condition," in *Proc. 21st Int. Conf. Elect. Mach. Syst.*, 2018, pp. 2460–2464, doi: 10.23919/ICEMS.2018.8549511.

[21] Z. Zhang et al., "A DC offset reduction of neutral point voltage strategy based on vector phase angle difference optimization for Vienna rectifier with bipolar DC bus," *IEEE Trans. Ind. Electron.*, vol. 71, no. 8, pp. 8313–8323, Aug. 2024, doi: 10.1109/TIE.2023.3325554.

[22] S. Xie, Y. Sun, M. Su, J. Lin, and Q. Guang, "Optimal switching sequence model predictive control for three-phase Vienna rectifiers," *IET Electr. Power Appl.*, vol. 12, pp. 1006–1013, 2018, doi: 10.1049/iet-epa.2018.0033.

[23] Y. Wang, J.-W. Yang, W.-J. Kim, T.-H. Kwon, T. Lee, and S.-J. Park, "Second harmonic current suppression and dynamic response improvement for V2G system," *IEEE Trans. Power Electron.*, vol. 38, no. 8, pp. 9566–9580, Aug. 2023, doi: 10.1109/TPEL.2023.3275575.

Yipei Wang (Member, IEEE) received the B.S. degree in smart grid information engineering and the M.S. degree in electrical engineering from the Qingdao University of Science and Technology, Qingdao, China, in 2017 and 2020, respectively, and the Ph.D. degree in electrical engineering from Chonnam National University, Gwangju, South Korea, in 2024.

From March to December 2024, he was a Postdoctoral Researcher with Chonnam National University, Gwangju, South Korea. Since January 2025, he has been with the Institute of Automation, Qilu University of Technology (Shandong Academy of Sciences), Jinan, China, as an Assistant Professor. His research interests include dc–dc converters, ac–dc converters, power conversion systems for electric vehicles, and applications for battery charger converters.

Sang-Hyeok Lee received the Ph.D. degree in electrical engineering from Chonnam National University, Gwangju, South Korea, in 2012.

From 2016 to 2022, he was a Deputy General Manager with Future Technology Research Laboratory, KyungShin, South Korea. He is currently a Principal Researcher with Smart Electrics Research Center, Korea Electronics Technology Institute, Gwangju, South Korea. His current research interests include mobility power conversion system and high-power EV charger.

Hyeon-Uk Go was born in South Korea in 1999. He received the B.S. degree from Honam University, Gwangju, South Korea, in 2018. He is currently working toward the M.S. degree with Chonnam National University, Gwangju, South Korea.

His research interests include power electronics, dc–dc converters, dc–ac inverters, and electric vehicle charging system applications.

Min-Seong Kim was born in South Korea in 2000. He received the B.S. degree from the Department of Electric Vehicle Engineering, Dongshin University, Naju, South Korea, in 2023. He is currently working toward the M.S. degree in electrical engineering with Chonnam National University, Gwangju, South Korea.

His research interests include ac–dc converters and control of power converters for electric vehicles.

Guangxu Zhou was born in Shandong, China. He received the B.S., M.S., and Ph.D. degrees in electrical engineering from the Shenyang University of Technology, Shenyang, China, in 1999, 2003, and 2006, respectively.

Since 2008, he has been a Research Professor with the Shandong Provincial Key Laboratory of Automotive Electronics Technology, Institute of Automation, Qilu University of Technology (Shandong Academy of Sciences), Jinan, China.

Sung-Jun Park (Member, IEEE) received the B.S., M.S., and Ph.D. degrees in electrical engineering and the Ph.D. degree in mechanical engineering from Pusan National University, Busan, South Korea, in 1991, 1993, 1996, and 2002, respectively.

He was an Assistant Professor with the Department of Electrical Engineering, Koje College, Geoje, South Korea, from 1996 to 2000, and the Department of Electrical Engineering, Tongmyong College, Busan, from 2000 to 2003. Since 2003, he has been a Professor with the Department of Electrical Engineering, Chonnam National University, Gwangju, South Korea. From 2007 to 2013, he was the Head of the Energy Power Center of Samsung Electro-Mechanics, Gwangju, South Korea. From 2018 to 2020, he was the CEO of G&EPS, Gwangju, South Korea. His research interests include renewable energy, ESS, electric vehicle-related converters and inverters, power conversion devices, motor driver design and control, battery charge/discharge converter, wireless charging and energy economics, trend prediction, and statistical data analysis. He is a member of the KIEE, KIPE, and KIIEE. Since 2019, he has been serving as the President of the Korean Society of Industry Convergence.